Article:
Delvenne, J-F orcid.org/0000-0002-1990-9738, Scally, B, Bunce, D orcid.org/0000-0003-3265-2700 et al. (1 more author) (2021) Splenium tracts of the corpus callosum degrade in old age. Neuroscience Letters, 742. 135549. ISSN 0304-3940

https://doi.org/10.1016/j.neulet.2020.135549

Splenium tracts of the corpus callosum degrade in old age

Jean-Francois Delvenne, Brian Scally, David Bunce, Melanie Rose Burke

School of Psychology, University of Leeds, U.K.

Correspondance to Jean-Francois Delvenne

Email: j.f.delvenne@leeds.ac.uk

Address (all authors):
School of Psychology,
Faculty of Medicine and Health,
University of Leeds,
Leeds, LS2 9JT
United Kingdom

Ackowledgments

This study was supported by research grant ARUK-PPG2014A-19 from Alzheimer's Research UK (ARUK). These findings were reported as part of a PhD thesis submitted by Brian Scally to the University of Leeds on 12th September 2018.

Keywords

Corpus Callosum; Splenium; Diffusion tensor imaging; Ageing

Abstract

It is well established that the posterior region of the corpus callosum, known as the splenium, is relatively preserved during the course of normal ageing. However, the effect of age on its distinct interhemispheric tract bundles that project to bilateral occipital, parietal and temporal areas of the cortex, is largely unknown. In the present study, diffusion tensor imaging was used to directly examine the integrity of these distinct segregations and their diffusion metrics were compared between groups of young adults (n = 20, mean age = 30.75) and older adults (n = 19, mean age = 80.21). Results revealed that while occipital tracts were preserved in older adults, parietal and temporal segments were particularly impaired. These findings are the first to indicate the existence of selective alterations in the posterior region of the corpus callosum in older age.

1. Introduction

It is widely accepted that the human corpus callosum (CC) exhibits an anterior-posterior gradient of degeneration with advancing age [1]. Specifically, normal ageing seems to target the small-diameter commissural tracts of the anterior CC genu, that project to bilateral areas of the frontal cortex [2, 3]. This is consistent with age-related cognitive decline in frontally-localised functions such as task switching [4], declarative memory [5] and problem solving [6]. In contrast, the CC splenium, which occupies the posterior region of the CC, appears to be relatively preserved in older age [7, 8].

While the 'splenium' label is typically applied to the posterior quarter of the midsagittal CC, the white matter fibres that pass through this region are diverse, such that they project bilaterally to three distinct brain regions: the occipital, parietal and temporal lobes [9-11]. Additionally, the distinct fibre bundles vary in diameter, from thin late-myelinating parietal fibres to large-diameter tracts connecting primary and extrastriate visual areas [11]. Inter-individual variability in the morphology of the CC suggests that region of interest (ROI) measures of the total splenium area are likely to be noisy, and as such the splenium should be functionally parcellated according to the topography of the commissural fibres for the most accurate measurements [12]. The choice of parcellation scheme directly determines which tracts contribute to the splenium ROI (see [13] for a review of parcellation schemes). Currently, no given parcellation scheme is able to account for inter-individual differences in the topography of the CC tracts, which is particularly evident in the splenium [10]. We have therefore developed a novel parcellation scheme in the current study, to address this issue in the literature.

The aim of the present study, therefore, was to investigate the effect of age on the distinct splenium tract bundles. DTI tractography [14] was used to reconstruct the white

matter pathways that traverse the splenium in the CC. Splenium tracts that connect bilateral occipital, parietal and temporal areas were segregated using our parcellation scheme. Their diffusion metrics were compared between groups of young and older adults to determine whether specific tract bundles varied according to age. Various parameters can be extracted from DTI that provide important insights in the present context. *Mean Diffusivity* (MD) describes the average magnitude of diffusivity within a voxel. Correlations between diffusion metrics and *in vitro* histological properties suggest that high MD reflects atrophy of axons, dendrites and myelin density [15]. *Radial Diffusivity* (RD) measures diffusion along the axis perpendicular to the direction of general diffusivity. RD has been significantly correlated with myelination and fibre density as measured by histological staining [16, 17]. *Axial Diffusivity* (AD) quantifies diffusion along the axis parallel to the direction of general diffusivity. Disruption to AD suggests atrophy of the axon (also known as Wallerian degeneration [16]). Finally, *Fractional Anisotropy* (FA) is probably the most commonly employed DTI metric and describes the general degree of anisotropy, or directionality dependence, within a voxel. Higher values of FA and AD indicate greater white matter integrity, whereas MD and RD are inverse measures, where higher values reflect lower integrity.

Previous research has suggested that age-related compensatory recruitment of brain activity in a given region is associated with reduced white matter integrity in the same region (the "less wiring more firing" hypothesis [18]). There is evidence of age-related compensatory activity in bilateral parietal and temporal regions [19, 20], and evidence of age-related cognitive decline in parietal and temporal functions, such as visuospatial working memory [21], spatial learning [22] and dichotic listening [23]. We therefore hypothesised that white matter integrity would be compromised in the splenium projections to parietal and temporal regions in older adults. We also

hypothesised that occipital tracts would be spared in older age, consistent with preserved interhemispheric processing of visual information in older adults [24].

2. Materials and methods

2.1. Participants

The data were collected and provided with permission by the Cambridge Centre for Ageing and Neuroscience (CamCAN) database [25, 26] (available at http://www.mrc-cbu.cam.ac.uk/datasets/camcan/). CamCAN is funded by the UK Biotechnology and Biological Sciences Research Council (grant number BB/H008217/1), with the support of the UK Medical Research Council and University of Cambridge, UK. Twenty older adults of more than 75 years old of age and 20 young adults of less than 40 years old of age were identified. Edinburgh Handedness Inventory [27] scores were used to select only fully right-handed participants for the present study (i.e., score of 100). One participant (male, age 85) was omitted from the analysis as parietal tracts could not be detected. The final groups consisted of 20 younger adults (mean age = 30.75, SD = 4.7, range = 23-37, females = 10) and 19 older adults (mean age = 80.21, SD = 2.89, range = 76-86, females = 10). All participants were classified as being cognitively healthy (MMSE > 24), monolingual (English), and free from neurological disease and psychiatric conditions (see [25] for a more detailed description of the exclusion criteria). A general vascular burden score, which represents the number of cardiovascular risk factors present for each participant, was calculated (see [28] for a similar approach). Five cardiovascular risk factors were identified and included hypertension (systolic blood pressure ≥140 mm Hg and/or diastolic blood pressure ≥90 mm Hg), obesity (body mass index ≥30), high blood cholesterol (self-report), diabetes (self-report of taking medication to treat diabetes), and smoking status (ever vs never). Across all participants, vascular burden was minimal

(younger adults: mean score = 0.9 out of 5, SD = 0.72, range = 0-2; older adults: mean score = 1.37 out of 5, SD = 0.91, range = 0-3). The ID codes, age, gender, years of education, cardiovascular risk factors, and vascular burden scores of the participants are shown in Appendix A. Ethical approval was obtained from the Cambridgeshire Research Ethics Committee and all participants gave their written informed consent before participation.

2.2. DTI acquisition and pre-processing

All participants were scanned for at least ten minutes using a 3T Siemens TIM Trio scanner. Diffusion weighted images were acquired using an echo-planar imaging sequence (30 directions for b-values of 1000 and 2000 s/mm^2, 3 scans at b = 0, TR = 9100 ms, TE = 104 ms, voxel size = 2 mm isotropic, FOV = 192 mm^2, 66 axial slices, averages = 1) (see [25, 26] for detailed parameters). DTI data were pre-processed with tools from the FMRIB Software Library (FSL; FMRIB Analysis Group, Oxford, UK). The DTI images were skull-stripped using the Brain Extraction Tool (BET). Corrections for eddy-current-induced distortions were made using the EDDY tool.

2.3. DTI Tractography

Whole brain probabilistic constrained spherical deconvolution tractography [29] was carried out using the ExploreDTI software. An angular threshold of 45° and FA contrast threshold of 0.2 was applied to all reconstructed tracts. ROIs were drawn onto the DTI scans of each participant to isolate the occipital, temporal and parietal tract bundles that pass through the splenium. Firstly, the splenium was identified by drawing a ROI on the middle slice of the sagittal plane around the posterior quarter of the entire CC (Figure 1-A). The tracts passing through this section were drawn to visualise the different bundles (Figure 1-B). For the occipital tracts, two ROIs were drawn on the

coronal plane to isolate the tracts projecting to the occipital lobe of each hemisphere, omitting tracts that projected to parietal areas (Figure 1-C & 1-D). Parietal tracts were selected by replacing the former ROIs surrounding the occipital tracts with new ROIs (Figure 1-E). Two more ROIs were drawn on sagittal planes left and right of the midline, to exclude tracts that projected to temporal areas (Figure 1-F). Parietal tracts are illustrated in Figure 1-G. Tracts that passed through the initial splenium ROI and projected forward to temporal areas were isolated with ROIs in the right and left hemisphere on coronal plane (Figure 1-H & 1-I).

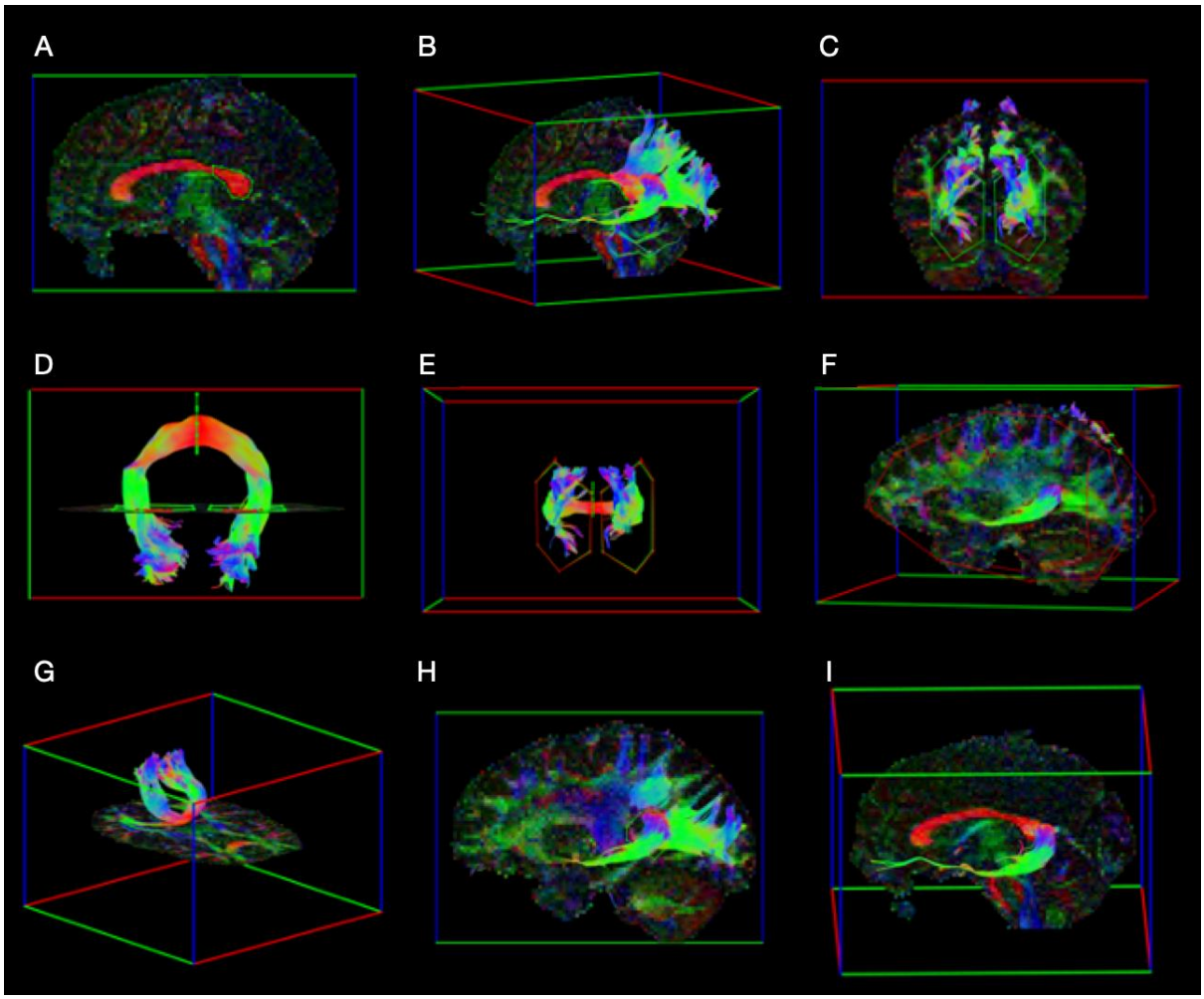

Figure 1: Sagittal view of ROI drawn around the splenium on the midsagittal scan (A). Sagittal view of all tracts traversing the midsagittal ROI (B). Rear coronal view of ROIs drawn around left and right occipital tract bundles (C). Axial view of interhemispheric occipital tracts, which are coloured according to direction (red: left-right; blue: top-bottom; green: front-back) (D). Rear coronal view of parietal ROIs (red) that exclude occipital ROIs (green) (E). Sagittal parietal ROIs drawn either side of the midline to exclude temporal tracts (F). The resulting interhemispheric parietal tracts (G). Sagittal ROIs drawn around left and right temporal projections from the splenium (H). The isolated interhemispheric temporal tracts (I).

Average FA, MD, RD, and AD metrics were extracted from these tracts of interest and used as dependent variables in the analyses. We segmented each callosal bundle ±6mm (three 2mm slices) either side of the sagittal midline to analyse the midsagittal segments of the CC, and to control for potential confounding effects of tract length or density [30].

2.4. Statistical analyses

We used a series of GLM Univariate ANCOVAs for each DTI measure (FA, MD, AD, and RD), with age group (young, older) as the independent variable to test for age group differences in the DTI parameters at each level of ROI. We included vascular burden, gender and years of education as the covariates. For display purposes, MD, AD and RD values were scaled by a factor of 10^3. In additon, we also ran linear regressions to test for possible relationships between the DTI parameters and four different factors: gender as an independent variable, with age, vascular burden, and years of education as continuous variables. The factor of age was considered as a continuous variable in the regression

analyses because of the relatively large age range in each group (i.e., 23-37 years for the group of young adults, and 76-86 years for the group of older adults).

3. Results

The results of the ANCOVAs, shown in Table 1 and Figure 2[1], reveal that older adults exhibited significantly greater MD, AD and RD in the parietal and temporal segments, and lower temporal FA in comparison to young adults. The analysis of DTI parameters for the occipital segments showed no significant differences between young and older adults.

ROI	DTI Metric	Mean Young	*SD* Young	Mean Older	*SD* Older	*F*	df	*p*	n_p^2
Occipital	FA	0.719	0.051	0.714	0.068	0.011	(1,34)	.916	<0.000
	MD	0.533	0.033	0.560	0.051	2.447	(1,34)	.127	0.067
	AD	1.086	0.073	1.126	0.071	4.035	(1,34)	.053	0.106
	RD	0.257	0.040	0.275	0.063	0.350	(1,34)	.558	0.010
Parietal	FA	0.619	0.051	0.602	0.074	0.078	(1,34)	.782	0.002
	MD	0.552	0.031	0.609	0.062	12.540	(1,34)	.001	0.269
	AD	1.011	0.059	1.089	0.087	15.329	(1,34)	<.001	0.311
	RD	0.322	0.038	0.370	0.070	4.792	(1,34)	.036	0.124
Temporal	FA	0.756	0.067	0.710	0.057	5.192	(1,34)	.029	0.132
	MD	0.507	0.037	0.565	0.042	23.502	(1,34)	<001	0.409
	AD	1.074	0.090	1.135	0.083	5.513	(1,34)	.025	0.140
	RD	0.223	0.048	0.280	0.049	12.619	(1,34)	.001	0.271

Table 1: Between-group analysis of segmented tract bundles

[1] The data has been reviewed and verified independently by reviewers

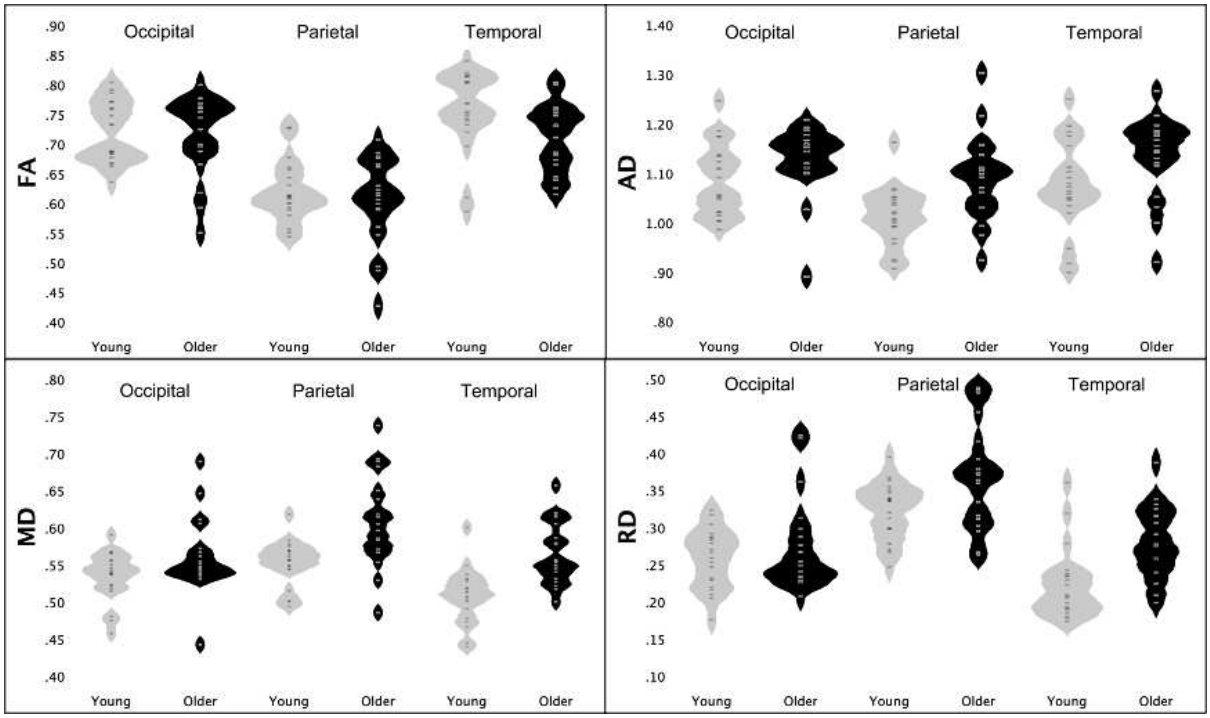

Figure 2: Violin plots illustrating the distribution of FA, AD, MD and RD values across the segmented splenium tracts in young and older adults. Each dot represents an individual participant.

Multiple linear regressions were then carried out to test if age, gender, vascular burden, and years of education were significant predictors of the DTI values (see appendix B). It was found that age was the main significant predictor of a number of DTI values: parietal MD (Beta = .535, p = .002), temporal MD (Beta = .645, p < .001), parietal AD (Beta = .561, p = .001), temporal AD (Beta = .364, p = .027), parietal RD (Beta = .356, p = .042), temporal RD (Beta = .548, p = .001), and temporal FA (Beta = -.376, p = .033). Gender also appears to account for some of the variability of the MD and AD values in the temporal tracts (Beta = .298, p = .024 and Beta = .364, p = .019, respectively), with females having greater variability in those values. Vascular burden was a significant predictor of the parietal AD values only (Beta = -.328, p = .041). Years of education was not a significant factor on any of the DTI values. Therefore, from these analyses, it remains clear

that age is the main variable that could explain the small amount of the variance in the DTI values in our participants.

4. Discussion

This cross-sectional study aimed to test whether distinct tract bundles of the CC splenium differed according to age. The analyses of the diffusion parameters of the white matter tract bundles that pass through the CC splenium showed that differential spatial patterns of degeneration occur in older age. The main findings from these analyses revealed that older adults had significantly increased MD and RD (thus, lower white matter integrity) in parietal and temporal tracts compared to young adults, while diffusivity of occipital segments was equivalent between the groups. Interestingly, older adults were also found to have higher AD than young adults in parietal and temporal tracts. As mentioned earlier, increased AD is consistent with greater diffusivity along the axon. This increase in older adults may therefore reflect continued axonal maturation in older age that coincides with reductions in MD and RD-based integrity, which has been linked to myelination [17]. Similar patterns have been reported in the CC genu, fornix and external capsule [6, 31, 32]. White matter structures that exhibit age-related increases in RD and AD have also been found to be structures that show the largest between-group differences in RD [31]. It has been suggested that areas that exhibit simultaneous RD/AD increases may be areas that suffer from age-induced reductions of axonal packing density (i.e., contain fibres of thin diameter), which could drive increases in AD [31]. In line with this hypothesis, studies of fibre composition of the CC indicate that parietal and temporal projections through the CC are thinner in diameter than occipital fibres [9, 33], which may explain why, in the present study, AD was greater in older adults for parietal and temporal tract segments, but not for occipital tract segments.

These novel findings support our hypothesis that older adults would experience integrity reductions in splenium connections that project to the areas of cortex that tend to be functionally disrupted during healthy ageing (i.e., the parietal and temporal areas). Indeed, a number of studies have provided evidence of age-related cognitive decline in parietal and temporal functions, such as visuospatial working memory [21], spatial learning [22] and dichotic listening [23]. However, to our knowledge, no studies have explicitly investigated the link between parietal and temporal tract bundles and cognitive decline in older age, so the functional implications of decline in these tracts remains unknown. Further investigations of possible functions attributed to these tracts are necessary to understand how these changes in white matter integrity may be important for cognitive decline. Our study also showed that the integrity of tracts projecting to the occipital cortices was retained in older adults. Occipital tracts are thought to support the transfer of visual information between the two cerebral hemispheres. This finding of preserved integrity in splenium connections that project to the occipital cortices is consistent with our previous demonstration of preserved interhemispheric processing of visual information in older adults [24].

We have interpreted age differences in the microstructural properties of reconstructed white matter tracts as a difference in the "integrity" of the targeted white matter fibres. Given the context of the study and the assumption that white matter microstructure does indeed deteriorate with age [34], this interpretation is justified. This finding has been demonstrated and discussed previously [30], and current thinking suggests that changes in the microstructural tract properties estimated by DTI may reflect phenomena other than integrity, such as tract density, axon diameter and the presence of crossing tracts (where two or more tracts are imaged within the same voxel). In the present study, we attempted to address this potential limitation by adjusting for

the approximate density of reconstructed tracts. Crossing tracts can lead to the distortion of the tensor model in a given voxel, especially when the crossing tracts diverge in orientation [35], rendering the interpretation of anisotropy and diffusion metrics redundant. As demonstrated previously, the splenium predominantly consists of voxels with a single (sagittal) fibre orientation, especially in midsagittal segments [35]. Our analysis of the mid-sagittal portion of the posterior CC should therefore have reduced the likelihood of estimating microstructural properties at the locations of crossing tracts.

5. Conclusions

To summarise, this study identified age-related modulations of the white matter tracts that pass through the splenium of the CC. These modulations suggest a reduction of integrity in the underlying white matter fibres in older age, likely due to demyelination as proposed by prior histological investigations of ageing [34]. To our knowledge, this is the first study to reveal that older adults experience poorer integrity in midsagittal parietal and temporal commissural segments of the splenium, while the midsagittal occipital segments are preserved. There is a need for longitudinal research to confirm these findings. Furthermore, very little research has considered these tracts in isolation, and their functional significance is relatively unknown. Further research is required to identify cognitive tasks that are facilitated by interhemispheric parietal and temporal tracts, and to what degree these tasks are affected by healthy normal ageing.

Conflicts of interest

The authors declare that the research was conducted in the absence of any commercial or financial relationships that could be construed as a potential conflict of interest.

References

[1] Lebel, C., Gee, M., Camicioli, R., Wieler, M., Martin, W., & Beaulieu, C. (2012). Diffusion tensor imaging of white matter tract evolution over the lifespan. *NeuroImage*, *60*(1), 340–352. http://doi.org/10.1016/j.neuroimage.2011.11.094

[2] Davis, S. W., Kragel, J. E., Madden, D. J., & Cabeza, R. (2012). The architecture of cross-hemispheric communication in the aging brain: Linking behavior to functional and structural connectivity. *Cerebral Cortex*, *22*(1), 232–242. http://doi.org/10.1093/cercor/bhr123

[3] Pfefferbaum, A., Adalsteinsson, E., & Sullivan, E. V. (2005). Frontal circuitry degradation marks healthy adult aging: Evidence from diffusion tensor imaging. *NeuroImage*, *26*(3), 891–899. http://doi.org/10.1016/j.neuroimage.2005.02.034

[4] Wasylyshyn, C., Verhaeghen, P., & Sliwinski, M. J. (2011). Aging and Task Switching: A Meta-Analysis. *Psychology and Aging*, *26*(1), 15–20. http://doi.org/10.1037/a0020912

[5] Rosen, A. C., Prull, M. W., O'Hara, R., Race, E. A., Desmond, J. E., Glover, G. H., … Gabrieli, J. D. E. (2002). Variable effects of aging on frontal lobe contributions to memory. *NeuroReport*, *13*(18), 2425–2428. http://doi.org/10.1097/00001756-200212200-00010

[6] Zahr, N. M., Rohlfing, T., Pfefferbaum, A., & Sullivan, E. V. (2009). Problem solving, working memory, and motor correlates of association and commissural fiber bundles in normal aging: A quantitative fiber tracking study. *NeuroImage*, *44*(3), 1050–1062. http://doi.org/10.1016/j.neuroimage.2008.09.046

[7] Fran, Q., Tian, Q., Ohringer, N. A., Nummenmaa, A., Witzel, T., Tobyne, S. M., et al. (2019). Age-related alterations in axonal microstructure in the corpus callosum measured by high-gradient diffusion MRI. *Neuroimage, 191*, 325-336. https://doi.org/10.1016/J.NEUROIMAGE.2019.02.036

[8] Ota, M., Obata, T., Akine, Y., Ito, H., Ikehira, H., Asada, T., & Suhara, T. (2006). Age-related degeneration of corpus callosum measured with diffusion tensor imaging. *NeuroImage*, *31*(4), 1445–1452. http://doi.org/10.1016/j.neuroimage.2006.02.008

[9] Aboitiz, F., Scheibel, A. B., Fisher, R. S., & Zaidel, E. (1992). Fiber composition of the human corpus callosum. *Brain Research*, *598*(1–2), 143–153. http://doi.org/10.1016/0006-8993(92)90178-C

[10] Hofer, S., & Frahm, J. (2006). Topography of the human corpus callosum revisited-Comprehensive fiber tractography using diffusion tensor magnetic resonance imaging. *NeuroImage*, *32*(3), 989–994. http://doi.org/10.1016/j.neuroimage.2006.05.044

[11] Knyazeva, M. G. (2013). Splenium of corpus callosum: Patterns of interhemispheric interaction in children and adults. *Neural Plasticity*, *2013*, 639430. http://doi.org/10.1155/2013/639430

[12] Westerhausen, R., Grüner, R., Specht, K., & Hugdahl, K. (2009). Functional relevance of interindividual differences in temporal lobe callosal pathways: A DTI tractography study. *Cerebral Cortex*, *19*(6), 1322–1329. http://doi.org/10.1093/cercor/bhn173

[13] Gooijers, J., & Swinnen, S. P. (2014). Interactions between brain structure and behavior: The corpus callosum and bimanual coordination. *Neuroscience and Biobehavioral Reviews*, *43*, 1–19. http://doi.org/10.1016/j.neubiorev.2014.03.008

[14] Johansen-Berg, H., & Behrens, T. E. J. (2006). Just pretty pictures? What diffusion tractography can add in clinical neuroscience. *Current Opinion in Neurology*.

http://doi.org/10.1097/01.wco.0000236618.82086.01
[15] Seehaus, A., Roebroeck, A., Bastiani, M., Fonseca, L., Bratzke, H., Lori, N., ... Galuske, R. (2015). Histological validation of high-resolution DTI in human post mortem tissue. *Frontiers in Neuroanatomy*, *9*. http://doi.org/10.3389/fnana.2015.00098
[16] Song, S. K., Sun, S. W., Ramsbottom, M. J., Chang, C., Russell, J., & Cross, A. H. (2002). Dysmyelination revealed through MRI as increased radial (but unchanged axial) diffusion of water. *NeuroImage*, *17*(3), 1429–1436. http://doi.org/10.1006/nimg.2002.1267
[17] Wei, P. T., Leong, D., Calabrese, E., White, L., Pierce, T., Platt, S., & Provenzale, J. (2013). Diffusion tensor imaging of neural tissue organization: Correlations between radiologic and histologic parameters. *Neuroradiology Journal*, *26*(5), 501–510. http://doi.org/10.1177/197140091302600502
[18] Daselaar, S. M., Iyengar, V., Davis, S. W., Eklund, K., Hayes, S. M., & Cabeza, R. E. (2015). Less wiring, more firing: Low-performing older adults compensate for impaired white matter with greater neural activity. *Cerebral Cortex*, *25*(4), 983–990. http://doi.org/10.1093/cercor/bht289
[19] Grady, C. L., McIntosh, A. R., Horwitz, B., & Rapoport, S. I. (2000). Age-related changes in the neural correlates of degraded and nondegraded face processing. *Cognitive Neuropsychology*, *17*(1–3), 165–186. http://doi.org/10.1080/026432900380553
[20] Maguire, E. A. (2003). Aging affects the engagement of the hippocampus during autobiographical memory retrieval. *Brain*, *126*(7), 1511–1523. http://doi.org/10.1093/brain/awg157
[21] De Jager, C. A., Milwain, E., & Budge, M. (2002). Early detection of isolated memory deficits in the elderly: The need for more sensitive neuropsychological tests. *Psychological Medicine*, *32*(3), 483–491. http://doi.org/10.1017/S003329170200524X
[22] Yamamoto, N., & DeGirolamo, G. J. (2012). Differential effects of aging on spatial learning through exploratory navigation and map reading. *Frontiers in Aging Neuroscience*, *4*(JUN), 1–7. http://doi.org/10.3389/fnagi.2012.00014
[23] Hommet, C., Mondon, K., Berrut, G., Gouyer, Y., Isingrini, M., Constans, T., & Belzung, C. (2010). Central auditory processing in aging: The dichotic listening paradigm. *Journal of Nutrition, Health and Aging*, *14*(9), 751–756. http://doi.org/10.1007/s12603-010-0097-7
24 [24] Scally, B., Burke, M. R., Bunce, D., & Delvenne, J. F. (2018). Visual and visuomotor interhemispheric transfer time in older adults. *Neurobiology of Aging*, *65*, 69–76. http://doi.org/10.1016/j.neurobiolaging.2018.01.005
[25] Shafto, M. A., Tyler, L. K., Dixon, M., Taylor, J. R., Rowe, J. B., Cusack, R., … Matthews, F. E. (2014). The Cambridge Centre for Ageing and Neuroscience (Cam-CAN) study protocol: A cross-sectional, lifespan, multidisciplinary examination of healthy cognitive ageing. *BMC Neurology*, *14*(1), 204. http://doi.org/10.1186/s12883-014-0204-1
[26] Taylor, J. R., Williams, N., Cusack, R., Auer, T., Shafto, M. A., Dixon, M., … Henson, R. N. (2017). The Cambridge Centre for Ageing and Neuroscience (Cam-CAN) data repository: Structural and functional MRI, MEG, and cognitive data from a cross-sectional adult lifespan sample. *NeuroImage*, *144*(Pt B), 262–269. http://doi.org/10.1016/j.neuroimage.2015.09.018
[27] Oldfield, R. C. (1971). The assessment and analysis of handedness: the Edinburgh inventory. *Neuropsychologia*, *9*(1), 97-113. https://doi.org/10.1016/0028-

3932(71)90067-4
[28] Williams, O. A., An, Y., Beason-Held, L., Huo, Y., Ferrucci, L., Landman, B. A., & Resnick, S. M. (2019). Vascular burden and APOE ε4 are associated with white matter microstructural decline in cognitively normal older adults. Neuroimage, 188, 572-583. https://doi.org/10.1016/J.NEUROIMAGE.2018.12.009
[29] Jeurissen, B., Leemans, A., Jones, D. K., Tournier, J. D., & Sijbers, J. (2011). Probabilistic fiber tracking using the residual bootstrap with constrained spherical deconvolution. *Human Brain Mapping*, *32*(3), 461–479. http://doi.org/10.1002/hbm.21032
[30] Jones, D. K., Knösche, T. R., & Turner, R. (2013). White matter integrity, fiber count, and other fallacies: The do's and don'ts of diffusion MRI. *NeuroImage*. http://doi.org/10.1016/j.neuroimage.2012.06.081
[31] Bennett, I. J., Madden, D. J., Vaidya, C. J., Howard, D. V., & Howard, J. H. (2010). Age-related differences in multiple measures of white matter integrity: A diffusion tensor imaging study of healthy aging. *Human Brain Mapping*, *31*(3), 378–390. http://doi.org/10.1002/hbm.20872
[32] Sullivan, E. V., Adalsteinsson, E., & Pfefferbaum, A. (2006). Selective age-related degradation of anterior callosal fiber bundles quantified In vivo with fiber tracking. *Cerebral Cortex*. http://doi.org/10.1093/cercor/bhj045
[33] Caminiti, R., Carducci, F., Piervincenzi, C., Battaglia-Mayer, A., Confalone, G., Visco-Comandini, F., … Innocenti, G. M. (2013). Diameter, Length, Speed, and Conduction Delay of Callosal Axons in Macaque Monkeys and Humans: Comparing Data from Histology and Magnetic Resonance Imaging Diffusion Tractography. *Journal of Neuroscience*, *33*(36), 14501–14511. http://doi.org/10.1523/JNEUROSCI.0761-13.2013
[34] Peters, A. (2002). The effects of normal aging on myelin and nerve fibers: A review. *Journal of Neurocytology*. http://doi.org/10.1023/A:1025731309829
[35] Jeurissen, B., Leemans, A., Tournier, J. D., Jones, D. K., & Sijbers, J. (2013). Investigating the prevalence of complex fiber configurations in white matter tissue with diffusion magnetic resonance imaging. *Human Brain Mapping*, *34*(11), 2747–2766. http://doi.org/10.1002/hbm.22099

Appendix A – participant codes and characteristics from CamCAN dataset (for replication)

ID	GROUP	AGE	GENDER	YEARS of EDUCATION	BMI	SYSTOLIC BLOOD PRESSURE (mmHg)	DIASTOLIC BLOOD PRESSURE (mmHg)	HIGH BLOOD CHOLESTEROL	DIABETES	SMOKING STATUS	VASCULAR BURDEN SCORE
CC110098	Younger	23	Male	17	NK	NK	NK	No	No	Ever	1
CC110319	Younger	28	Female	20	24.23	104	50.5	No	No	Never	0
CC120264	Younger	28	Male	16	20.93	108.5	74.5	No	No	Ever	1
CC120727	Younger	23	Female	21	23.58	125.5	87	No	No	Never	0
CC121194	Younger	24	Female	18	25.20	111.5	77	No	No	Ever	1
CC121317	Younger	25	Female	21	31.64	113.5	71.5	No	No	Ever	2
CC121397	Younger	27	Male	22	25.79	121.5	82.5	No	No	Ever	1
CC210422	Younger	34	Male	22	21.38	122.5	79	No	No	Ever	1
CC210526	Younger	37	Male	25	23.37	113	84.5	No	No	Ever	1
CC220132	Younger	31	Male	18	21.45	139	93	No	No	Ever	2
CC220223	Younger	33	Male	24	25.13	117	74	No	No	Ever	1
CC220635	Younger	36	Female	26	33.22	106	81	No	No	Ever	2
CC220806	Younger	35	Female	22	17.66	103	62.5	No	No	Never	0
CC220828	Younger	33	Female	22	21.27	111	66.5	No	No	Never	0
CC221033	Younger	28	Female	21	23.37	95	58	No	No	Never	0
CC221040	Younger	36	Male	18	24.32	115.5	74.5	No	No	Ever	1
CC221580	Younger	31	Female	18	35.65	111	73	No	No	Ever	2
CC221977	Younger	37	Male	25	23.71	113	78	No	No	Ever	1
CC222125	Younger	34	Male	24	21.27	103	67	No	No	Never	0
CC222956	Younger	32	Female	16	25.18	108	71	No	No	Ever	1
CC610146	Older	76	Female	27	NK	NK	NK	No	No	Ever	1
CC610212	Older	77	Female	17	30.64	122	79	No	No	Ever	2
CC610658	Older	78	Male	23	33.28	136	81.5	No	No	Never	1
CC620572	Older	78	Female	23	30.16	132.5	86.5	No	No	Ever	2
CC620610	Older	76	Male	26	26.81	166.5	79	No	No	Never	1
CC710099	Older	85	Female	24	NK	NK	NK	No	No	Ever	1
CC710350	Older	81	Male	21	29.23	109.5	59	No	No	Ever	1
CC710548	Older	83	Male	15	NK	NK	NK	No	No	Ever	1
CC711128	Older	80	Male	14	30.16	123	55.5	Yes	No	Ever	3
CC720188	Older	78	Male	25	29.87	174	81.5	Yes	No	Ever	3
CC720290	Older	84	Male	21	19.87	115	62.5	No	No	Ever	1

CC720400	Older	86	Female	15	21.55	136	73	Yes	No	Ever	2
CC720511	Older	79	Male	24	31	137.5	85.5	No	No	Ever	2
CC720622	Older	81	Female	22	25.68	142	61.5	No	No	Ever	2
CC721107	Older	79	Female	21	24.36	128	67.5	No	No	Ever	1
CC721504	Older	82	Male	26	26.32	122.5	56	No	No	Never	0
CC721648	Older	80	Female	25	26.25	136	72	No	No	Never	0
CC721704	Older	82	Female	22	22.80	148	77.5	No	No	Never	1
CC722421	Older	79	Female	20	25.50	162.5	88.5	No	No	Never	1

Appendix B – Results of the linear regression analyses

	Gender				Age				Vascular Burden				Years of Education			
ROI & DTI metric	**B**	**95% CI**	**Beta**	**p**	**B**	**95% CI**	**Beta**	**p**	**B**	**95% CI**	**Beta**	**p**	**B**	**95% CI**	**Beta**	**p**
Occipital																
FA	.-.004	[-.043, .034]	-.037	.818	<.001	[-.001, .001]	.031	.860	-.021	[-.047, .006]	-.283	.118	.003	[-.003, .009]	.167	.330
MD	.015	[-.014, .044]	.168	.310	<.001	[<.001, .001]	.234	.186	.007	[-.013, .027]	.122	.497	.001	[-.005, .004]	-.042	.808
AD	.033	[-.014, .079]	.225	.162	.001	[<.001, .002]	.300	.082	-.021	[-.053, .012]	-.223	.203	.001	[-.006, .008]	.052	.754
RD	.007	[-.027, .041]	.067	.681	<.001	[-.001, .001]	.083	.634	.018	[-.005, .042]	.277	.126	-.002	[-.007, .003]	-.116	.498
Parietal																
FA	.015	[-.027, .056]	.117	.483	<.001	[-.001, .001]	-.041	.816	-.021	[-.049, .008]	-.262	.153	-.001	[-.008, .005]	-.078	.655
MD	.003	[-.031, .036]	.023	.875	.001	[<.001, .002]	.535	.002	-.007	[-.030, .016]	-.096	.555	<.001	[-.005, .005]	-.007	.965
AD	.024	[-.023, .071]	.146	.310	.002	[-.001, .003]	.561	.001	-.034	[-.067, .-001]	-.328	.041	-.002	[-.009, .006]	-.067	.654
RD	-.008	[-.047, .030]	-.068	.671	.001	[<-.010, .002]	.356	.042	.007	[-.020, .033]	.092	.599	.001	[-.005, .006]	.037	.827
Temporal																
FA	.008	[-.034, .050]	.064	.689	-.001	[-.002, .<001]	-.376	.033	.002	[-.027, .031]	.025	.888	.004	[-.003, .010]	.190	.262
MD	.029	[.004, .053]	.298	.024	.001	[.001, .002]	.645	.<.001	-.008	[-.025, .009]	-.127	.361	-.002	[-.005, .002]	-.113	.398
AD	.065	[.011, .119]	.364	.019	.001	[<.001, .002]	.364	.027	-.017	[-.054, .021]	-.146	.372	.001	[-.007, .009]	.032	.839
RD	.010	[-.022, .043]	.093	.526	.001	[.001, .002]	.548	.001	-.003	[-.026, .019]	-.048	.764	-.003	[-.008, .002]	-.174	.260